Brain, Behavior, and Immunity 35 (2014) 86–95

Contents lists available at ScienceDirect

Brain, Behavior, and Immunity

journal homepage: www.elsevier.com/locate/ybrbi

Brain protein expression changes in WAG/Rij rats, a genetic rat model of absence epilepsy after peripheral lipopolysaccharide treatment

Balázs Györffy [a], Zsolt Kovács [b], Péter Gulyássy [a], Attila Simor [a], Katalin Völgyi [a], Gergely Orbán [a], Péter Baracskay [a], Zoltán Szabó [c], Tamás Janáky [c], Árpád Dobolyi [d], Gábor Juhász [a], András Czurkó [a,c], Katalin A. Kékesi [a,e,*]

[a] Laboratory of Proteomics, Institute of Biology, Eötvös Loránd University, Pázmány P. stny. 1/c, Budapest H-1117, Hungary
[b] Department of Zoology, The University of West Hungary, Savaria Campus, Károlyi Gáspár tér 4, Szombathely H-9700, Hungary
[c] Institute of Medical Chemistry, University of Szeged, Dóm tér 8, Szeged H-6720, Hungary
[d] Semmelweis University and the Hungarian Academy of Sciences, Department of Anatomy, Histology and Embryology, Neuromorphological and Neuroendocrine Research Laboratory, Tüzoltó utca 58, Budapest H-1094, Hungary
[e] Department of Physiology and Neurobiology, Eötvös Loránd University, Pázmány P. stny. 1/c, Budapest H-1117, Hungary

ARTICLE INFO

Article history:
Received 2 May 2013
Received in revised form 2 September 2013
Accepted 2 September 2013
Available online 8 September 2013

Keywords:
Brain proteomics
Epilepsy
Inflammation
LPS
NFkB
Sleep–wake cycle

ABSTRACT

Peripheral injection of bacterial lipopolysaccharide (LPS) facilitates 8–10 Hz spike-wave discharges (SWD) characterizing absence epilepsy in WAG/Rij rats. It is unknown however, whether peripherally administered LPS is able to alter the generator areas of epileptic activity at the molecular level. We injected 1 mg/kg dose of LPS intraperitoneally into WAG/Rij rats, recorded the body temperature and EEG, and examined the protein expression changes of the proteome 12 h after injection in the fronto-parietal cortex and thalamus. We used fluorescent two-dimensional differential gel electrophoresis to investigate the expression profile. We found 16 differentially expressed proteins in the fronto-parietal cortex and 35 proteins in the thalamus. It is known that SWD genesis correlates with the transitional state of sleep–wake cycle thus we performed meta-analysis of the altered proteins in relation to inflammation, epilepsy as well as sleep. The analysis revealed that all categories are highly represented by the altered proteins and these protein-sets have considerable overlap. Protein network modeling suggested that the alterations in the proteome were largely induced by the immune response, which invokes the NFkB signaling pathway. The proteomics and computational analysis verified the known functional interplay between inflammation, epilepsy and sleep and highlighted proteins that are involved in their common synaptic mechanisms. Our physiological findings support the phenomenon that high dose of peripheral LPS injection increases SWD-number, modifies its duration as well as the sleep–wake stages and decreases body temperature.

1. Introduction

The integrity of mammalian organisms is controlled by two regulatory supersystems: the immune system and the nervous system (Elenkov et al., 2000). A fascinating example of neuro-immune interactions is the relationship between inflammatory processes and epileptogenesis, which represents an intensively studied field of neuro-immunology (Lee et al., 2008; Maroso et al., 2010; Vezzani et al., 2011a,b). Elevated proinflammatory cytokine level can enhance epileptic seizure susceptibility (Galic et al., 2008; Shandra et al., 2002; Vezzani et al., 2008a), as increased serum cytokine levels are found in several different epilepsy syndromes (Sinha et al., 2008). These proinflammatory cytokines are shown to be synthesized by the glial cells in the brain (Mlodzikowska-Albrecht et al., 2007; Vezzani et al., 2008a,b) and a fine balance exists between excitatory and inhibitory neurotransmitters and between pro- and anti-inflammatory cytokines (Devinsky et al., 2013).

Bacterial lipopolysaccharide (LPS) is responsible for inflammatory reactions associated with Gram-negative bacterial infections. We previously reported that WAG/Rij (Wistar Albino Glaxo/Rijswijk) rats (Coenen and van Luijtelaar, 2003; van Luijtelaar and Coenen, 1986) – a genetic rat model of absence epilepsy – responded to both peripheral (Kovács et al., 2006) and central (Kovács et al., 2011) LPS administration with enhanced seizure activity, as reflected by high amount of 8–10 Hz spike and wave discharges (SWDs), which represent the electrophysiologically detectable

* Corresponding author at: Laboratory of Proteomics, Institute of Biology, Eötvös Loránd University, Pázmány P. stny. 1/c, Budapest H-1117, Hungary. Tel.: +36 1 3722500; fax: +36 1 3812204.
E-mail addresses: kakekesi@dec001.geobio.elte.hu, kakekesi@caesar.elte.hu (K.A. Kékesi).

0889-1591/$ - see front matter © 2013 Elsevier Inc. All rights reserved.
http://dx.doi.org/10.1016/j.bbi.2013.09.001

state of seizures in absence epilepsy. However, the mechanism by which peripheral LPS cause central effects in the brain is not well known. On the cellular level, LPS is expected to induce changes in protein expression, triggered by its binding to Toll-like receptor 4 (TLR4) (Laflamme and Rivest, 2001; Li and Verma, 2002; Singh and Jiang, 2004). Through the toll-ceramide pathway, it invokes the nuclear factor-kappaB (NFkB) transcription factor, thereby activating hundreds of genes (Beutler, 2004; Bonizzi and Karin, 2004; Pahl, 1999; Singh and Jiang, 2004). Moreover, TLR4 activation triggers the synthesis and release of cytokines, e.g., IL1β (Kuno and Matsushima, 1994; Li and Verma, 2002; Vezzani et al., 2011b) Thereafter, the activated interleukin receptors – in the plasma membrane of certain neurons and astrocytes – are able to induce a signaling cascade, which also leads to NFkB activation (Li and Verma, 2002; Vezzani et al., 2011b). Thus, both LPS and LPS-induced interleukin release have a common final target in the transcription factor, NFkB. Whereas an avalanche of genes can be transcribed in the brain after peripheral LPS injection (Godbout et al., 2005; Singh and Jiang, 2004), only a particular fraction of a given set of transcribed genes are translated into proteins (Gygi et al., 1999); therefore, understanding the molecular mechanisms of altered excitability on the protein expression level after peripheral LPS injection is an important issue.

If there is an increase in the endogenous cytokine release, evoked by the immune response, it influences the sleep–wake behavior (Lorton et al., 2006; Opp, 2005; Opp et al., 2007) and changes the electrical activity of the brain (Shandra et al., 2002). Indeed, LPS administration changes the sleep-wake cycle in rats, increases slow wave sleep (SWS) and decreases wakefulness and rapid eye movement (REM) sleep (Kapás et al., 1998; Krueger et al., 1986; Schiffelholz and Lancel, 2001). Additionally, correlations between the sleep–wake cycle and the occurrence of SWDs in WAG/Rij rats have been revealed: high numbers of SWDs were found during light SWS and lower SWD numbers were detected during active wakefulness, deep SWS and REM sleep (Coenen et al., 1991; Drinkenburg et al., 1991). Thus, these data suggest that the inflammation induced alterations in vigilance are in a tight connection with the increased seizure genesis.

From a broad perspective, LPS-induced seizure enhancement in WAG/Rij rats is an easily reproducible and advantageous model for studying inflammation-related changes in the brain proteome. As SWDs in WAG/Rij rats are generated in the thalamo-cortical neuronal circuits (Suffczynski et al., 2004), we examined the fronto-parietal cortex and thalamus. The changes in the cortical and thalamic proteome after peripheral LPS application were studied by fluorescent two-dimensional differential gel electrophoresis (2D-DIGE), and the results were extensively analyzed by Ariadne Genomics' Pathway Studio® literature-based protein network modeling software. We found changes in both the cortical and thalamic proteome in conjunction with the LPS treatment of WAG/Rij rats and revealed their connections with inflammation, epilepsy and sleep-wake cycle alterations.

2. Methods

2.1. EEG experiment

2.1.1. Implantation of animals for EEG recording

Six-month-old WAG/Rij rats were used in all experiments. Animals were kept under a 12-h light–dark cycle (light was on from 08.00 AM to 08.00 PM), and food and water were supplied *ad libitum*. The care and treatment of all animals conformed to guidelines approved by Council Directive 86/609/EEC and the Hungarian Act of Animal Care and Experimentation (1998, XXVIII), as well as with local regulations for the care and use of animals for research. Rats were maintained in air-conditioned rooms at 22 ± 2 °C, and all efforts were taken to minimize the animals' pain and suffering and to reduce the number of animals used.

In the electrophysiological experiment, five rats were implanted while under Halothane-air mixture (1%) anesthesia with 0.8-mm stainless steel screw electrodes for EEG recording as described previously (Kovács et al., 2006). Briefly, screw electrodes were placed into the bone above the frontal (A 2.0, L 2.1) and parietal (A −6.5, L 2.1) cortices (Paxinos and Watson, 1997). The ground electrode was placed above the cerebellar cortex, whereas a stainless steel reference electrode (a plate of 3 × 4 mm) was implanted under the skin and over the masseter muscle. Electrodes were soldered to a ten-pin socket and glued to the skull with dentacrylate cement. Lidocaine ointment was used for post-implantation pain relief. Rats were allowed to recover for at least two weeks. The recovery was controlled by recording the EEG, and full recovery was established when the SWD frequency was stabilized. Animals were gently handled several times daily to reduce stress-induced changes in the SWD-number. Thermo-resistors (Pt 100) were used for body temperature measurement by implanting them onto the surface of the skull. Body temperature was measured every 10 min at 0.05 °C accuracy with a thermometer (SUPERTECH Ltd., Pécs, Hungary).

2.1.2. Recording of SWDs and LPS treatments

A differential amplifier (SUPERTECH Bioamp 4, Pécs, Hungary) and an analog–digital conversion interface (CED 1401 μII data capture and analysis device; Cambridge, UK) were used for EEG data recording (bandwidth of the EEG recording: 0.3–150 Hz, sampling rate: 1 kHz). To establish the average SWD numbers, average SWD duration and total duration of SWDs, as well as the sleep–wake pattern, animals ($n = 5$) were i.p. injected daily with 1 ml saline for 3 days and EEGs were recorded. Following the 3-day control period, rats were i.p. injected with 1 mg/kg LPS (Sigma–Aldrich Ltd., Budapest, Hungary, *Escherichia coli*, serotype O111:B4) dissolved in 1 ml saline. To examine the possible long-lasting effects of LPS on SWDs and the sleep–wake cycle, a saline control experiment (post-treatment control day, 1 ml saline i.p.) was performed on the fifth day.

The same dose of LPS was injected into intact WAG/Rij rats ($n = 6$) for the proteomic study.

2.1.3. Analysis of EEG data: determination of SWD numbers and SWD duration and evaluation of sleep-wake stages

We measured the number and duration of SWDs, as well as the sleep–wake stages, between 30 and 270 min post-injection (from 1.30 PM to 6.00 PM). Initial stress can change the number of SWDs and the sleep–wake stages in the first 30 min (Kovács et al., 2006, 2012; Sarkisova and van Luijtelaar, 2011); thus, the first 30-min post-injection time was omitted from analysis. The recording periods were split into 60-min sections, and these sections were evaluated separately. SWDs (with the average amplitude at least twice as high as the basal EEG activity, power spectra 7–11 Hz) (Fig. 1A) were extracted from the raw data files and were checked by FFT analysis (Kovács et al., 2006).

EEG was analyzed offline by visual evaluation of the raw EEG (Gottesmann et al., 1995; Kovács et al., 2006, 2012). Briefly, we distinguished five stages in 60-min epochs as follows: passive awake (dominantly beta (20–40 Hz) and theta (6–8 Hz) activity); active awake (beta and theta activity interrupted by high slow waves of motor artifacts); light slow-wave sleep (light SWS; sleep spindles (10–16 Hz), theta waves and some slow waves (2–4 Hz)); deep slow-wave sleep (deep SWS; gradually disappearing sleep spindles and increasing ratio of high slow delta waves (0.5–4 Hz)); and rapid eye movement sleep (REM sleep; continuous theta activity without any motor artifact).

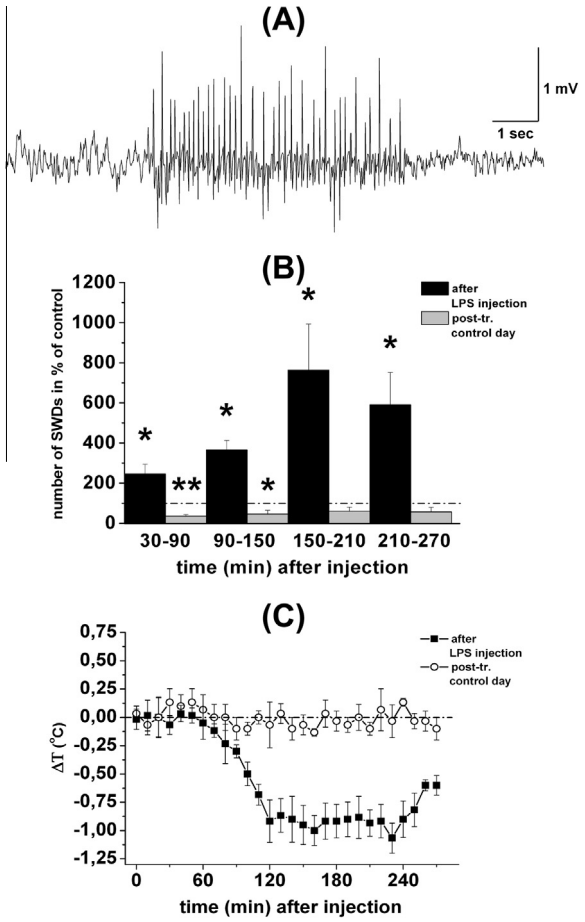

Fig. 1. The effect of 1 mg/kg LPS (i.p.) on the epileptic activity and body temperature of WAG/Rij rats. (A) A representative SWD measured in the WAG/Rij rat. (B) Number of SWDs after LPS injection (black columns) and on the following day (post-treatment control day: post-tr. control day; gray columns) in the% of control. The number of SWDs significantly increased during the whole 4-h recording period after the LPS treatment, whereas on the post-treatment control day it significantly decreased between 30 and 150 min; * labels $p < 0.05$ and ** labels $p < 0.005$ level of significance. (C) Changes of the body temperature (°C) after LPS injection (black squares) and on the post-treatment control day (post-tr. control day; open circles).

The means of averaged SWD number, SWD duration and duration of sleep-wake stages of 3-day control periods were compared to the SWD number, SWD duration and duration of sleep-wake stages measured after i.p. LPS injection and on the post-treatment control day. The changes were evaluated by ANOVA.

2.2. Proteomics experiment

2.2.1. Preparation of tissue samples and the DIGE method

The gender, the weight and the age of rats were the same in the proteomics and the electrophysiological experiments. The two studies were done at different time and on different animals, but in the same schedule. Animals used in the proteomics experiment were i.p. injected daily with 1 ml saline for 3 days. After 3 days, LPS or saline injection in LPS treated or control groups of animals were done at the same time points in both experiments. The LPS-treated rats ($n = 6$) and saline-injected control rats ($n = 6$) were sacrificed 12 h after injections and the brains were rapidly removed from the skull (<20 s) and immediately cooled in dry ice. The thalamus and the fronto-parietal cortex were dissected on a plate in dry ice and stored at −80 °C until use. Alteration of protein expression profile was determined using 2D-DIGE Minimal Dye method. All equipment, material and software were supplied from GE Healthcare, Little Chalfont, UK, if not, it is labeled separately. The detailed DIGE protocol has been described in our earlier study (Szego et al., 2010). In briefly, after brain homogenization and centrifugation protein concentration was determined. Fifty micrograms of protein containing volume of the samples was labeled with CyDye DIGE Fluor Minimal Labeling Kit. Brain lysates from LPS- or saline-treated rats were labeled with Cy3 or Cy5 randomly, and the reference (pooled internal standard) was labeled with Cy2. The three differently labeled protein samples were multiplexed and six mixtures were run in six gels simultaneously. The isoelectric focusing was performed on 24-cm IPG strips (pH 3–10 NL) in an Ettan IPGphor instrument. After separation the focused proteins were reduced then alkylated in equilibrating buffer containing mercaptoethanol and iodoacetamide, respectively for 20–20 min (both of them were purchased from Sigma–Aldrich Ltd., Budapest, Hungary). Then the strips were loaded onto 10% polyacrylamide gels (24 × 20 cm) and electrophoresis was performed using an Ettan DALT System. Following electrophoresis, gels were scanned in a TyphoonTRIO+ scanner using appropriate lasers and filters. Differences were visualized using Image Quant software and quantitative analysis was performed using the DeCyder software package: the Differential In-gel Analysis and the Biological Variance Analysis modules. The p values (Student's t-test) were determined for each protein spot. The internal standard was a pool of equal amounts of all samples within the experiment, and it was representative of every protein present and was the same across all gels. The standard provided an average image against which all other gel images were normalized, thus removing much of the experimental variation and reducing gel-to-gel variation.

For protein identification, a separate preparative 2D electrophoresis was performed with the above mentioned methods and settings using a total of 800 μg of proteins per gel. Resolved protein spots were visualized post-electrophoretically by Colloidal Coomassie Blue G-250 (Merck, Darmstadt, Germany) according to the protocol.

Individual spots of interest were punched out from the preparative gel, de-stained and subjected to in-gel digestion with trypsin (Trypsin Gold (Promega)) for 8 h at 37 °C (modified after Shevchenko et al., 1996). Tryptic digest peptides were extracted from gel pieces using 5% formic acid and were dried under a vacuum.

2.2.2. LC/MS analysis and protein identification

All LC-MS experiments were performed using Agilent 1100 Series nano-LC coupled through an orthogonal nanospray ion source to an Agilent LC-MSD XCT Plus ion trap mass spectrometer (Agilent Co., USA). The nano-LC system was operated in sample enrichment/desalting mode using a ZORBAX 300SB-C18 column (0.3 × 50 mm, 5 μm) for the enrichment and a ZORBAX 300SB-C18 (75 μm × 150 mm) nanocolumn for the chromatography. Elution of peptides was accomplished by gradient elution at a flow rate of 300 nl/min with a gradient from 100% solvent A (0.1% formic acid in water) to 40% solvent B (0.1% formic acid in acetonitrile) in 25 min. The MS was operated in peptide scan auto-MS/MS mode, acquiring full-scan MS spectra (300–1600 m/z) at a scan speed of 8100 u/s and a resolution of less than 0.35 u (FWHM). From the four most abundant peaks in the MS spectrum, automated, data-dependent MS/MS was used to collect MS/MS spectra (100–1800 m/z at 26,000 u/s and a resolution of less than 0.6 u, FWHM).

All acquired data were processed and peak lists were generated by the Agilent DataAnalysis 3.2 software using the default settings. All MS/MS samples were analyzed using Mascot 2.2.04 (Matrix Science, London, UK) and X! Tandem http://www.thegpm.org/tandem/. Mascot and X! Tandem were set up to search the Swissprot 56.8 database, assuming trypsin as the digestion

enzyme. Both search engines assumed a fragment ion mass tolerance of 0.80 Da and a parent ion tolerance of 1.5 Da. An iodoacetamide derivative of cysteine as a fixed modification and oxidation of methionine as a variable modification were specified in Mascot and in X! Tandem.

Scaffold (version Scaffold_2_02_03, Proteome Software Inc., Portland, OR) was used to validate MS/MS-based peptide and protein identifications. Peptide identifications were accepted if they could be established at greater than 95.0% probability, and protein identifications were accepted with greater than 95.0% probability and containing at least 2 identified peptides.

2.2.3. Strategies of interpretation modeling

For interpretation of our proteomics data, we first used manual verification and initial functional clustering using PDB (http://www.pdb.org, La Jolla, CA, USA), ExPASy and UniProt databases (http://www.expasy.org and http://www.uniprot.org, respectively; Swiss Institute of Bioinformatics, Switzerland). Subsequently, the lists of altered proteins were given to the Ariadne Genomics Pathway Studio® 9.0 software environment, a protein interaction database and protein network modeling software (ResNet 9.0, 2010Q4, Ariadne Genomics, Inc, Rockville, MD, USA) (Kékesi et al., 2012). The group enrichment analysis tool was used to assign cellular localization to our measured proteins. We made two separate figures for the LPS effect in the two brain structures. We built two protein interaction pathways where NFkB and some NFkB-regulated proinflammatory proteins (chemokines, cytokines, enzymes and adhesion molecules) are connected to the altered proteins in our brain samples and are grouped according to the available literature. In these two figures, inflammation-related networks are shown, where connections represent LPS-induced alterations and connections between well-known, and recently identified, inflammation-related proteins.

We also tested whether our measured proteins could be found in the SynProt database (http://www.synprot.de), which is dedicated to synaptic proteins primarily based on data obtained from twelve different proteomics screens on postsynaptic density (PSD) synaptic protein preparations.

3. Results

3.1. Changes in the SWD number, SWD duration and body temperature after LPS injection

LPS injection (1 mg/kg i.p.) significantly increased the number of spike and wave discharges (SWDs) in WAG/Rij rats (Fig. 1B). One recorded example of SWDs, characterized by 8–10 Hz oscillations is shown on Fig. 1A. The number of SWDs more than doubled relative to the control level (246.6 ± 47.5%) in the first measured hour (30–90 min), and it increased further during the following 2 h (up to 763.5 ± 229.3%) and remained high (591.3 ± 161.1%) in the last hour (210–270 min; Fig. 1B). In addition, the total SWD duration also increased in parallel with an increase in the SWD number (in the% of control; 30–90 min: 257.4 ± 56.4; 90–150 min: 279.3 ± 25.6; 150–210 min: 568.6 ± 163.4; and 210–270 min: 524.4 ± 98.5). LPS injection also changed the morphology of the SWDs, as the amplitude of the SWDs became more variable and the long SWD spindles were fragmented. Indeed, the average SWD duration significantly decreased between 90–150 and 150–210 min (% of control: 78.5 ± 6.2 and 75.5 ± 6.6). On the post-treatment control day, the SWD number significantly decreased between 30–90 and 90–150 min (SWD number/SWD duration as% of control: 35.5 ± 9.1/31.2 ± 7.1 and 45.5 ± 19.0/44.6 ± 18.4). LPS caused a 1.0 degree Celsius decrease in body temperature during the second measured hour, which remained reduced for two hours, then started to increase, and on the post-treatment control day returned to normal (Fig. 1C).

3.2. Effect of LPS treatment on sleep-wake stages

The mean of active and passive wake time (sec) significantly decreased during the whole 4-h recording period after LPS treatment (except the passive wake time between 30 and 90 min), whereas light SWS duration significantly increased (% of control; 30–90 min: 135.0 ± 7.7; 90–150 min: 129.2 ± 5.6; 150–210 min: 130.9 ± 9.9; 210–270 min: 141.5 ± 6.5). Deep SWS and REM sleep times were significantly decreased by LPS between only 210–270 min (% of control; deep SWS: 83.2 ± 6.0; REM sleep: 67.1 ± 8.5).

We did not observe significant changes in sleep-wake stages on the post-treatment control days.

3.3. LPS altered the proteome of the fronto-parietal cortex and thalamus

We used 2D-DIGE proteomics technology to investigate the differences in the protein expression profile of the fronto-parietal cortex and thalamus of WAGR/Rij rats that were peripherally injected with LPS. Fifteen protein spots in the fronto-parietal cortex and 28 protein spots in the thalamus had significant differences (Suppl. Fig. 1 shows the representative gel images). The fold changes in the fluorescence intensities of the protein spots were in the ranges of −1.106 to −1.378 (reduced concentration) and +1.062 to +2.044 (elevated concentration) after the LPS treatment (groups were normalized to the internal standard), and all changes were statistically significant ($p < 0.05$) using standard t-test across all gels (see Suppl. Table 1). In the cortex, 8 protein spots' intensity increased while seven spots' intensity decreased in gel compared to the control after the LPS treatment. In the thalamus, 19 protein spots' intensity increased and nine spots' intensity decreased (see Suppl. Table 1).

MS/MS analysis of the altered spots revealed 16 proteins from the cortex and 35 proteins from the thalamus (Table 1, Suppl. Tables 1 and 2). The following four proteins were found in both brain areas: ATP synthase subunit d, mitochondrial protein (ATP5H), glyceraldehyde-3-phosphate dehydrogenase (GAPDH), glial fibrillary acidic protein (GFAP) and neurofilament light polypeptide (NEFL). The number of spots and the number of identified proteins cannot be matched directly, as there were a few spots without an identified protein, while in many cases, the same spot contained more than one protein. To determine high abundance proteins in a multi-protein spot, MS *mol%* is estimated from the exponentially modified protein abundance index (emPAI) calculated for each protein and the sum of emPAI values of all proteins in the spot (see Suppl. Table 1). Only peptides with scores above the homology threshold were counted (http://www.matrixscience.com/help/quant_empai_help.html). Only very low abundance proteins (<2 *mol%*) were removed, false positive expression changes are considered to be caused by random coincidence of isoelectric point (IEP) and molecular weight (Mw). Furthermore, there were proteins that were identified from multiple spots. In some exceptional cases, the same protein can be found in two different spots that changed in opposing directions (see Table 1 and Suppl. Table 1). These are common phenomena in gel-based proteomics, and they can be explained by the physical interactions of some proteins or by post translational modifications (e.g. phosphorylation).

Functional clustering revealed that the measured proteins could be associated with biological functions and processes, such as cytoskeletal proteins ($n = 11$; Th-Ctx; overlap: 10-3; 2), motor proteins ($n = 4$; 4-0; 0), chaperone/oxidative stress ($n = 6$; 5-1; 0), carbohydrate metabolism ($n = 4$; 3-2; 1), lipid metabolism ($n = 3$; 1-2; 0), protein metabolism ($n = 2$; 2-0; 0), ATP synthesis/respiratory chain

Table 1
Functionally clustered protein list and identification data of significantly altered proteins in the thalamus and the cortex. * proteins involved in synaptic functions.

Gene name	Protein name	Th	Ctx	Cellular localization	Function
Cytoskeletal proteins					
ACTA2*	Smooth muscle alpha-actin	↓		Cytoplasm	Cytoskeletal protein, cell motility
CAPG*	Macrophage-capping protein	↑		Cytoplasm, nucleus, extracellular space	Cytoskeletal organization, involved in macrophage function
DPYSL2*	Dihydropyrimidinase-related protein 2	↑		Cytoplasm, mitochondrion	Axon guidance, neuronal growth, cell migration, cytoskeleton remodeling
GFAP*	Glial fibrillary acidic protein	↑↓	↑	Cytoplasm	Cytoskeletal protein, cell-specific marker
INA*	Alpha-internexin	↑		Cytoplasm	Cytoskeletal organization, neuronal morphogenesis
LMNA*	Lamin-A	↓		Nucleus	Provides a framework for the nuclear envelope and interacts with chromatin
LMNB1*	Lamin-B1		↓	Nucleus	Provides a framework for the nuclear envelope and interacts with chromatin
NEFL*	Neurofilament light polypeptide	↓	↓	Cytoplasm	Maintenance of neuronal caliber
TUBB2A*	Tubulin beta-2A chain	↑		Cytoplasm	Microtubule-based movement
TUBB2C*	Tubulin beta-2C chain, Neuron-specific	↑		Cytoplasm	Microtubule-based movement
TUBB3*	Tubulin beta-3 chain	↑		Cytoplasm	Microtubule-based movement
Motor proteins					
MYH1	Myosin, heavy chain 1; skeletal muscle – Myh11 O08638	↓		Cytoplasm	Motor protein, muscle contraction
MYL1*	Myosin, light chain 1	↓		Cytoplasm	Motor protein, regulatory light chain of myosin
TAGLN2*	Transgelin 2	↓			Muscle organ development
TPM2*	Tropomyosin 2 (beta chain)	↑		Cytoplasm	Motor protein, association with the troponin complex
Chaperone/oxidative stress					
DNAJB11	DnaJ homolog subfamily B member 11	↑		Cytoplasm, endoplasmic reticulum	Co-chaperone for HSPA5
HSPA8*	Heat shock cognate 71 kDa protein		↑↓	Cytoplasm, plasma membrane	Chaperone
PARK7*	Protein DJ-1	↑		Cytoplasm, mitochondrion, nucleus	Chaperone, response to oxidative stress
PDIA6*	protein disulfide-isomerase 6	↑		Endoplasmic reticulum	Catalyzes the rearrangement of –S–S– bonds in proteins
STIP1	Stress-induced-phosphoprotein 1	↓		Cytoplasm, nucleus	Association of the molecular chaperones HSC70 and HSP90
PRDX6*	Peroxiredoxin 6	↑		Cytoplasm, endoplasmic reticulum	Response to oxidative stress, lipid metabolism
Carbohydrate metabolism					
ENO1*	Alpha-enolase	↑		Cytoplasm, nucleus, plasma membrane	Glycolysis, growth control, hypoxia tolerance, allergic responses
GAPDH*	Glyceraldehyde-3-phosphate dehydrogenase	↓	↑	Cytoplasm	Carbohydrate metabolism, tRNA binding, transcription regulation, apoptosis, cytoskeletal organization
MDH1*	Malate dehydrogenase, cytoplasmic	↑↓		Cytoplasm	Carbohydrate metabolism, glycolysis
TPI1*	Triosephosphate isomerase		↓	Cytoplasm	Glycolysis, gluconeogenesis
Lipid metabolism					
APOE*	Apolipoprotein E	↑		Extracellular space	Cytoskeleton organization, lipid metabolism, response to oxidative stress
IAH1	Isoamyl acetate-hydrolyzing esterase 1 homolog		↑	Cytoplasm	Lipid degradation
PAFAH1B2	Platelet-activating factor acetylhydrolase IB subunit beta		↑	Cytoplasm	Lipid degradation, lipid metabolism
Protein metabolism					
PSME1	Proteasome activator complex subunit 1		↑	Cytoplasm	Immunoproteasome assembly and antigen processing
UCHL1*	Ubiquitin carboxyl-terminal hydrolase isozyme L1	↑		Cytoplasm	Processing of ubiquitin precursors and of ubiquitinated proteins
ATP synthesis/respiratory chain					
ATP5B*	ATP synthase, H+ transporting, mitochondrial F1 complex, beta polypeptide	↑↓		Mitochondrion	ATP synthesis
ATP5H*	ATP synthase subunit d, mitochondrial	↓	↓	Mitochondrion	ATP synthesis
NDUFV2*	NADH dehydrogenase [ubiquinone] flavoprotein 2, mitochondrial	↑		Mitochondrion	Core subunit of the membrane respiratory chain NADH dehydrogenase
SUCLA2*	Succinyl-CoA ligase [ADP-forming] subunit beta, mitochondrial		↓	Mitochondrion	Carbohydrate metabolism, tricarboxylic acid cycle
UQCRC1*	Cytochrome b-c1 complex subunit 1, mitochondrial		↑	Mitochondrial inner membrane	Respiratory chain
Signal transduction					
GNB2*	Guanine nucleotide-binding protein G(I)/G(S)/G(T) subunit beta-2	↑		Cytoplasm	Modulator or transducer in various transmembrane signaling systems
GUK1*	Guanylate kinase 1		↓	Cytoplasm	Recycling GMP and indirectly, cGMP
Transcription/translation					
HNRNPA2B1*	Heterogeneous nuclear ribonucleoprotein A2/B1		↑	Nucleus	Pre-mRNA processing
HNRNPH2*	Heterogeneous nuclear ribonucleoprotein H2	↓		Nucleus	Pre-mRNA processing

Table 1 (*continued*)

Gene name	Protein name	Th	Ctx	Cellular localization	Function
PURA*	Transcriptional activator protein Pur-alpha	↑		Nucleus, cytoplasm	Transcription activation, initiation of DNA replication and recombination
Synaptic transmission					
ATP6V1E1*	V-type proton ATPase subunit E 1	↑↓		Lysosome, mitochondrion, plasma membrane	Acidifying a variety of intracellular compartments
NECAP1*	Adaptin ear-binding coat-associated protein 1	↓		Cytoplasm, plasma membrane	Involved in endocytosis
SEPT3*	Neuronal-specific septin-3	↑		Cytoplasm, plasma membrane	Synaptic plasticity, cytoskeletal filament formation cytokinesis
SEPT5*	Septin-5	↑		Cytoplasm, plasma membrane, synaptic vesicle membrane	Cytoskeleton organization, cytokinesis
SH3GL2*	Endophilin-A1		↑	Cytoplasm, mitochondrion	Recruition of proteins to membranes, synaptic vesicle endocytosis
Miscellaneous					
PPA1	Inorganic pyrophosphatase	↑		Cytoplasm	Phosphate metabolic process
VDAC1*	Voltage-dependent anion-selective channel protein 1		↑	Mitochondrion, plasma membrane	Cell volume regulation, apoptosis

($n = 5$; 3-3; 1), signal transduction ($n = 2$; 1-1; 0), transcription/translation ($n = 3$; 2-1; 0), synaptic transmission ($n = 5$; 4–1; 0) and miscellaneous ($n = 2$; 1-1; 0) (see Table 1).

To gain more biologically relevant information from our protein lists, we performed a literature-based bioinformatics analysis. By manual literature search, we sorted the experimentally altered proteins into groups based on their association with epilepsy and LPS-induced inflammation (Suppl. Table 3). We assigned the proteins to the following 4 groups: (i) proteins known both from the epilepsy and LPS literature (15 altered proteins); (ii) proteins known only from the literature on epilepsy (13); (iii) proteins known only from the LPS literature (10); and iv) proteins that are not known in either the LPS or epilepsy literature (10). The majority of the proteins (81%) were known from the extensive epilepsy and/or LPS-induced inflammation literature (Suppl. Table 3). Moreover, we also compiled a list of the sleep-related proteins (32, (68%)) (Suppl. Table 3) based on the sleep-promoting effect of LPS treatment to elucidate common cellular components of the processes involved in absence seizures and sleeping.

3.4. Interpretation modeling of our proteomics data

We compiled two separate figures for the LPS effect in the two brain structures (Fig. 2 and Fig. 3). In the modeling we marked the certainly identified proteins to separate them from the uncertain ones (based on Suppl. Table 1). We considered a protein "certainly identified" if (a) it was the only one found in a given spot; or (b) it had the highest MS *mol%* score in a multi-protein spot; or (c) two proteins in a single spot with the highest MS *mol%* scores if the difference between their scores was <5%. Some proteins revealed in our study are highly connected to members of the complex inflammation-related molecular network, and a notable proportion of the identified proteins are involved in these networks in general.

We also searched the SynProt database for the recently identified proteins, and forty of the measured proteins (85%) were found in the database as follows (see Table 1; (*) after gene name): thalamus 31 (66%), cortex 13 (28%), and both 4 (100%).

4. Discussion

We report here that peripherally injected LPS induces alterations in the cortical and thalamic brain tissue proteome of WAG/Rij rats that occur in parallel with enhanced epileptic spike-wave discharges, and we report the effects of LPS on the sleep-wake cycle. SWDs in the electroencephalogram (EEG) are the hallmark of absence seizures, reflecting hypersynchronization in thalamo-cortical circuits. Experimental studies of genetic rat models of absence epilepsy have indicated that the perioral region of the somatosensory (parietal) cortex initiates the seizure activity that entrains the thalamo-cortical circuit and produces generalized SWD activity (Meeren et al., 2002; Polack et al., 2007). No structural changes were observed in SWD generator brain regions, but several changes at the subcellular level have been observed, such as changes in receptor subunits (Beyer et al., 2008; van de Bovenkamp-Janssen et al., 2006) and ion channel expression (de Borman et al., 1999; Klein et al., 2004; Kole et al., 2007; Lakaye et al., 2002; van de Bovenkamp-Janssen et al., 2004; Weiergräber et al., 2008). Recently, a proteomics study identified ATP synthase subunit delta, 14-3-3 zeta isoform, myelin basic protein and macrophage migration inhibitory factor as differentially expressed proteins in these regions in Genetic Absence Epilepsy Rats from Strasbourg (GAERS) (Danis et al., 2011). Thus, it can be assumed that the seizure genesis areas in WAG/Rij rats are molecularly different from normal rats.

Previously, we demonstrated that both peripheral and central LPS injection facilitates SWD genesis in the WAG/Rij rat (Kovács et al., 2006, 2011). In this study, we injected a high dose of LPS (1 mg/kg i.p.) that increased the SWD number up to 800% and decreased the body temperature. In addition, the SWD number decreased on the post-treatment control day, indicating that protein expression changes reduced the absence-like activity. This finding suggests that SWDs are sensitive read-outs of molecular changes that enhance the thalamo-cortical excitability and hypersynchronization induced by LPS. Because protein synthesis and degradation are time consuming and because alterations in the proteome are more sustained than the changes in the transcriptome, we measured protein expression changes 12 h after LPS injection and identified 16 differentially expressed proteins in the fronto-parietal cortex and 35 proteins in the thalamus. Thus, we focused on sustained protein changes, which were sustained longer than the rapidly developing proinflammatory cytokine response to LPS. Proteomics is a principally data-driven molecular hypothesis-making approach; therefore, we intend to select molecular mechanisms that can be investigated by classical experimental approaches.

4.1. Critical considerations about the interpretation of proteomics data

Protein separation and detection methods are less sensitive than RNA detection due to a lack of amplification methods such

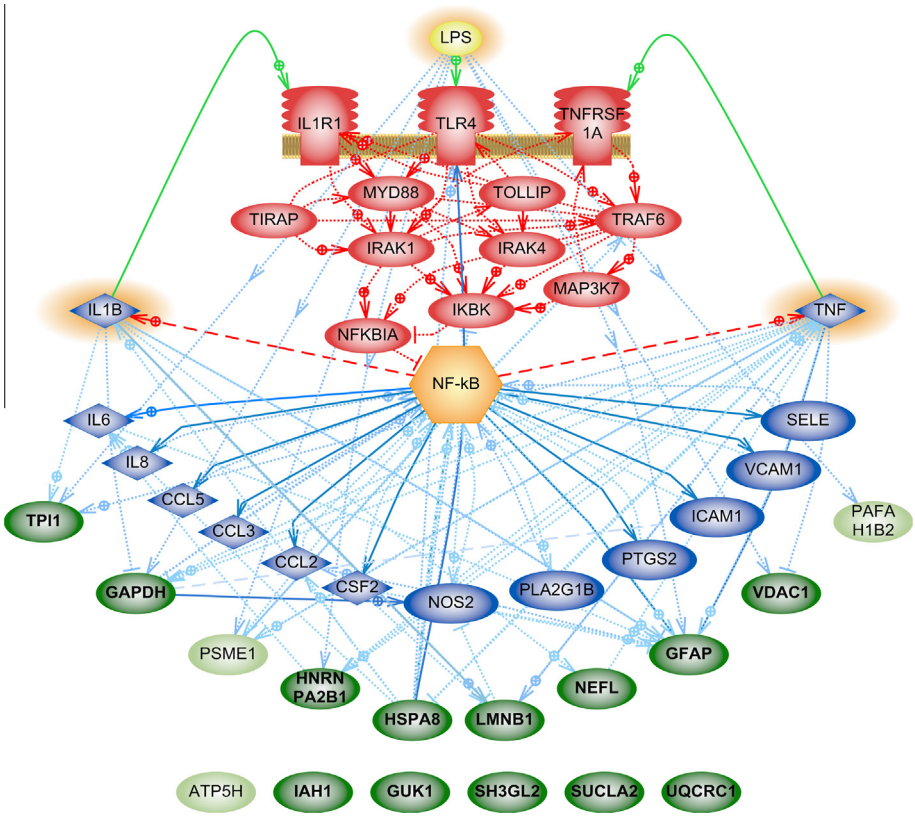

Fig. 2. Network of inflammation-related proteins supplemented with proteins identified from the cerebral cortex. The figure depicts that LPS induced signaling in the periphery leads to the subsequent production of proinflammatory factors (IL1B and TNF are highlighted) which activate proinflammatory cellular events as well and the latter occurs also in the central nervous system. Connections between the entities represent direct bindings, protein modifications and expression regulations. Red: Inflammation promoting proteins upstream to NF-κB. Blue: Inflammation promoting proteins downstream to NF-κB. Green: Proteins identified from the cerebral cortex. *Abbreviations:* CCL2: C–C motif chemokine 2; CCL3: C–C motif chemokine 3; CCL5: C–C motif chemokine 5; CSF2: granulocyte–macrophage colony-stimulating factor; ICAM1: intercellular adhesion molecule 1; IKBK: inhibitor of nuclear factor kappa-B kinase; IL1B: interleukin-1 beta; IL1R1: interleukin-1 receptor type 1; IL6: interleukin-6; IL8: interleukin-8; IRAK1: interleukin-1 receptor-associated kinase 1; IRAK4: interleukin-1 receptor-associated kinase 4; LPS: lipopolysaccharide; MAP3K7: mitogen-activated protein kinase kinase kinase 7; MYD88: myeloid differentiation primary response protein MyD88; NF-kB: nuclear factor NF-kappa-B; NFKBIA: NF-kappa-B inhibitor alpha; NOS2: nitric oxide synthase, inducible; PLA2G1B: phospholipase A2; PTGS2: prostaglandin G/H synthase 2; SELE: E-selectin; TIRAP: toll/interleukin-1 receptor domain-containing adapter protein; TLR4: Toll-like receptor 4; TNF: tumor necrosis factor; TOLLIP: toll-interacting protein; TRAF6: TNF receptor-associated factor 6; VCAM1: vascular cell adhesion protein 1. The certainly identified proteins marked with darker color and bold text, based on Suppl. Table 2. (For interpretation of the references to color in this figure legend, the reader is referred to the web version of this article.)

as PCR. Deduction of protein expression from mRNA would provide only a partial solution because of the intense mRNA degradation in the nucleus, as only a fraction of the transcribed genes are translated into proteins and the selection rules are unknown (Gygi et al., 1999). State-of-the-art proteome analysis allows the detection of a few thousand proteins (detecting 2000–3000 proteins is routine) out of the estimated 30,000 different proteins within a cell (Lopez, 2007; Marouga et al., 2005). Thus, we are only capable of tracking the concentration changes of 10% of the entire proteome of a sample. Therefore, it is not surprising that the primary dataset of the statistically significant protein concentration changes in a DIGE study contains a relatively small number of altered proteins, which are weakly interconnected by direct interactions.

Without a method capable of tracking the concentration changes of all proteins in a given cell, we have to deal not merely with our measured proteins but also with their known protein interactions. In the present study we tried to follow this logic as we attempted to highlight the complexity of the cellular processes that drive LPS-induced changes in brain function (and dysfunction) using bioinformatics tools for extending the measured dataset to functionally relevant networks of proteins that might be involved in the molecular action of LPS. Our approach was based on the reconstruction of known LPS-activated protein networks, such as the cytokine release inducing pathways. We used the Ariadne Genomics Pathway Studio® 9.0 software environment, which was developed for the analysis and navigation of molecular networks (Nikitin et al., 2003). It uses MedScan technology, which is a natural language processing engine that extracts molecular interactions and functional relationships from the entire contents of PubMed, as well as accessible open-source full-text articles (Novichkova et al., 2003). It has to be noted that Pathway Studio makes 10% false connections in a network, thus we performed a serious control of the network nodes and edges.

4.2. LPS administration-induced signaling leads to extensive metabolic changes – functional interplay between inflammation, sleep and epilepsy

The identified proteins that changed after LPS injection in the WAG/Rij rats were associated with several different cellular processes (see Table 1). The majority of the measured proteins were known from the extensive epilepsy and/or LPS/inflammation literature, and only eight altered proteins (17%) were found to be independent from both (4 are not shown in Suppl. Table 3). According to the literature, LPS-induced cellular changes involve receptors on the cell surface and a complex inflammation-related intracellular molecular network (see Figs. 2 and 3). The massive amount of the network-connected proteins, identified in our recent study, is

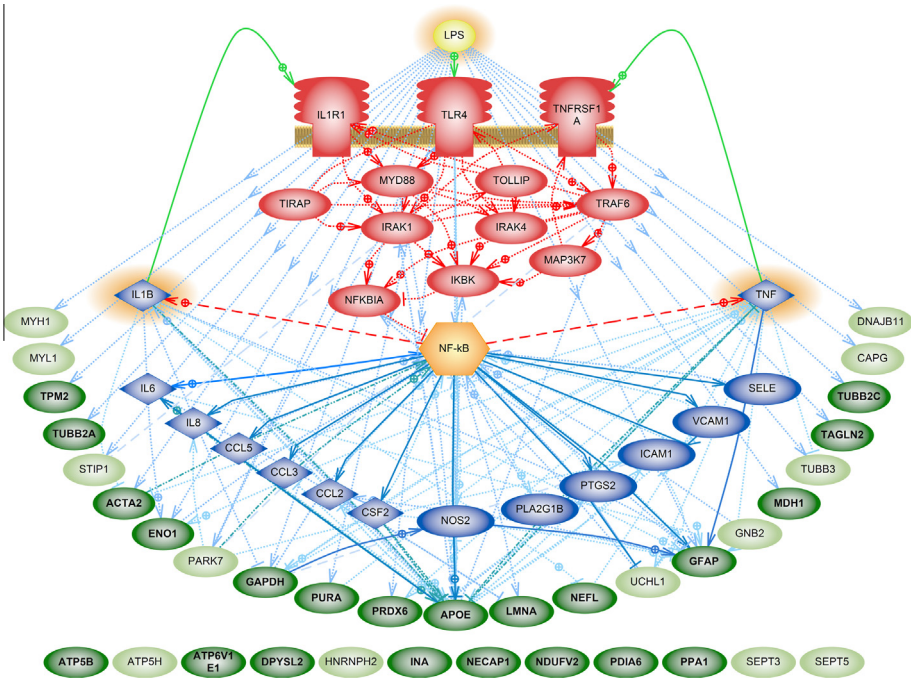

Fig. 3. Network of inflammation-related proteins supplemented with proteins identified from the thalamus. The figure depicts that LPS induced signaling in the periphery leads to the subsequent production of proinflammatory factors (IL1B and TNF are highlighted) which activate proinflammatory cellular events as well and the latter occurs also in the central nervous system. Connections between the entities represent direct bindings, protein modifications and expression regulations. Red: Inflammation promoting proteins upstream to NF-κB. Blue: Inflammation promoting proteins downstream to NF-κB. Green: Proteins identified from the thalamus. *Abbreviations:* CCL2: C–C motif chemokine 2; CCL3: C–C motif chemokine 3; CCL5: C–C motif chemokine 5; CSF2: granulocyte–macrophage colony-stimulating factor; ICAM1: intercellular adhesion molecule 1; IKBK: inhibitor of nuclear factor kappa-B kinase; IL1B: interleukin-1 beta; IL1R1: interleukin-1 receptor type 1; IL6: interleukin-6; IL8: interleukin-8; IRAK1: interleukin-1 receptor-associated kinase 1; IRAK4: interleukin-1 receptor-associated kinase 4; LPS: lipopolysaccharide; MAP3K7: mitogen-activated protein kinase kinase kinase 7; MYD88: myeloid differentiation primary response protein MyD88; NF-kB: nuclear factor NF-kappa-B; NFKBIA: NF-kappa-B inhibitor alpha; NOS2: nitric oxide synthase, inducible; PLA2G1B: phospholipase A2; PTGS2: prostaglandin G/H synthase 2; SELE: E-selectin; TIRAP: toll/interleukin-1 receptor domain-containing adapter protein; TLR4: Toll-like receptor 4; TNF: tumor necrosis factor; TOLLIP: toll-interacting protein; TRAF6: TNF receptor-associated factor 6; VCAM1: vascular cell adhesion protein 1. The certainly identified proteins marked with darker color and bold text, based on Suppl. Table 2. (For interpretation of the references to color in this figure legend, the reader is referred to the web version of this article.)

an interesting finding. The proteins associated with the epilepsy literature are mainly related to carbohydrate and energy metabolism, and the data assume intensive cytoskeletal changes as well (Suppl. Table 3). These facts led to a hypothesis about functional crosstalk between the molecular mechanisms of epilepsy and inflammation in the brain, and they support the idea that inflammation-activated signaling is able to influence metabolic activity and cytoskeletal alterations, which in turn are associated with enhanced epileptic seizures.

In addition, cytokines are responsible for inflammation-induced sleep enhancement (Krueger, 2008; Krueger et al., 1986, 2011) and increased seizure susceptibility (Vezzani, 2005; Vezzani et al., 2002, 2008a,b). Thus, it is also an interesting topic to elucidate the relationship between the modification of the sleep–wake cycle by LPS treatment and increased frequency of seizures. A 1 mg/kg dose of LPS increased the time of light SWS and decreased the deep SWS time, so the observed rise in SWD number could be a consequence of that change in vigilance. We conducted a literature-based bioinformatics analysis from the altered proteins in relation to sleep. From the 47 affected proteins, 32 (68%) were identified in the sleep literature (Suppl. Table 3), and among these proteins, 27 were known from the epilepsy and/or LPS/inflammation literature as well (Suppl. Table 3). Many of the sleep-related proteins were also involved in mechanisms of seizure generation, and only 5 of 32 were solely sleep-related proteins in our dataset. In conclusion, our data suggest overlapping molecular mechanisms of inflammation, sleep and epilepsy in the brain. LPS is assumed to be a factor in exerting a sleep-promoting effect; thus, the shift in the sleep–wake cycle to light SWS after LPS administration may enhance the occurrence of absence seizures. This is another data-driven working hypothesis that requires serious investigation in the future.

4.3. Proteomics data highlights proteins that are also involved in synaptic function

In our previous study, we measured the elevation of IL1β, TNFα and IL6 after injection of 350 μg/kg LPS in the WAG/Rij rat (Kovács et al., 2006), as an increase in cytokine levels is involved in direct synaptic modulation that influences the brain.

One of the most interesting findings of our proteomics study is that the majority of the altered proteins may be involved in synaptic transmission, as 85% of them have been found in the SynProt database (see * in Table 1).

Several proteins regulate synaptogenesis by their involvement in the formation of developing neurites and in the arborization of the dendritic structures, including alpha-internexin (INA) (Benson et al., 1996), dihydropyrimidinase-related protein 2 (DPYSL2) (Chae et al., 2009), neuronal specific septin-3 (SEPT3) (Tsang et al., 2011), septin-5 (SEPT5) (Tsang et al., 2011), and ubiquitin carboxyl-terminal hydrolase isozyme L1 (UCHL1) (Cartier et al., 2009). The following is another group of identified proteins that are known molecular players in the recycling of synaptic vesicles or in vesicular neurotransmitter filling: adaptin ear-binding coat-associated protein 1 NECAP1 (Murshid et al., 2006), endophilin-A1 (SH3GL2) (Sullivan, 2011), SEPT3 (Tsang et al., 2011), SEPT5 (Beites et al., 2005; Tsang et al., 2011), and V-type proton ATPase subunit E 1 (ATP6V1E1) (Di Giovanni et al., 2010; El Far and Seagar,

2011). DPYSL2 (Brittain et al., 2009) and neurofilament light polypeptide (NEFL) (Fiordelisio et al., 2007) are able to modulate voltage-gated calcium-channels; moreover, voltage-dependent anion-selective channel protein 1 (VDAC1) is also implicated in the regulation of intracellular Ca^{2+} homeostasis (Rapizzi et al., 2002), which is essential in synaptic events (e.g., exocytosis of synaptic vesicles). Apolipoprotein E (APOE) presumably influences synaptic plasticity (Herz and Chen, 2006). Finally, alpha-enolase (ENO1) (Ueta et al., 2004), glyceraldehyde-3-phosphate dehydrogenase (GAPDH) (Ikemoto et al., 2003; Schousboe et al., 2011), heat shock cognate 71 kDa protein (HSPA8) (Tobaben et al., 2001), and protein DJ-1 (PARK7) (Usami et al., 2011) are attached to certain parts of synaptic membranes, such as synaptic vesicles.

These data support our observation that the LPS administration induced immune response influences synaptic processes directly and causes increased seizure frequency, which was recorded 25–30 min after LPS injection. In turn, we can raise the third data-driven hypothesis for further research that LPS action in the brain has a synaptic effect, targeting the synaptic molecular network and inducing a rapid onset change in neurotransmission elicited by immune response related cytokine level elevation. This is an interesting hypothesis for further research because synaptic mitochondria are involved in seizure genesis (Folbergrová and Kunz, 2012).

The WAG/Rij model of absence epilepsy provides an excellent read-out for such changes and allows extensive investigation of synaptic functions in inflammation.

In conclusion, after high-dose LPS injection, we found alterations in the cortical and thalamic proteome of the WAG/Rij rat that occurred in parallel with increased seizure activity. The peripheral inflammatory response could induce remodeling of the brain proteome, and this remodeling could directly involve several proteins of the synaptic region. We suggest here three data-driven hypotheses for further studies on the influence of peripherally induced inflammation on brain functions. Our data suggest a complex and sustained change in the signaling system, mitochondrial metabolism and synaptic transmission after peripheral application of LPS that could be mainly driven by the immune reaction triggered elevation of cytokine levels in the brain.

Conflict of interest

All authors declare that there are no conflicts of interest.

Acknowledgments

This work was supported by Economic Competitiveness Operational Programme (GVOP-3.2.1.-2004-04-0309) to G. Juhász, Social Renewal Operational Programme (TÁMOP 4.2.1./B-09/1/KMR-2010-0003) to G. Juhász, A. Czurkó and K.A. Kékesi and by the Scientific Foundation of NYME SEK/NYME SEK TTK (2010–2011) Hungary and National Development Agency of Hungary (under Grant No. TIOP-1.3.1.-07/2-2F-2009-2008) to Zs. Kovács.

We wish to thank Tamás Török for the technical assistance.

Appendix A. Supplementary data

Supplementary data associated with this article can be found, in the online version, at http://dx.doi.org/10.1016/j.bbi.2013.09.001.

References

Beites, C.L., Campbell, K.A., Trimble, W.S., 2005. The septin Sept5/CDCrel-1 competes with alpha-SNAP for binding to the SNARE complex. Biochem. J. 385, 347–353.

Benson, D.L., Mandell, J.W., Shaw, G., Banker, G., 1996. Compartmentation of alpha-internexin and neurofilament triplet proteins in cultured hippocampal neurons. J. Neurocytol. 25, 181–196.

Beutler, B., 2004. Inferences, questions and possibilities in Toll-like receptor signalling. Nature 430, 257–263.

Beyer, B., Deleuze, C., Letts, V.A., Mahaffey, C.L., Boumil, R.M., Lew, T.A., Huguenard, J.R., Frankel, W.N., 2008. Absence seizures in C3H/HeJ and knockout mice caused by mutation of the AMPA receptor subunit Gria4. Hum. Mol. Genet. 17, 1738–1749.

Bonizzi, G., Karin, M., 2004. The two NF-kappaB activation pathways and their role in innate and adaptive immunity. Trends Immunol. 25, 280–288.

Brittain, J.M., Piekarz, A.D., Wang, Y., Kondo, T., Cummins, T.R., Khanna, R., 2009. An atypical role for collapsin response mediator protein 2 (CRMP-2) in neurotransmitter release via interaction with presynaptic voltage-gated calcium channels. J. Biol. Chem. 284, 31375–31390.

Cartier, A.E., Djakovic, S.N., Salehi, A., Wilson, S.M., Masliah, E., Patrick, G.N., 2009. Regulation of synaptic structure by ubiquitin C-terminal hydrolase L1. J. Neurosci. 29, 7857–7868.

Chae, Y.C., Lee, S., Heo, K., Ha, S.H., Jung, Y., Kim, J.H., Ihara, Y., Suh, P.G., Ryu, S.H., 2009. Collapsin response mediator protein-2 regulates neurite formation by modulating tubulin GTPase activity. Cell. Signal. 21, 1818–1826.

Coenen, A.M., Van Luijtelaar, E.L., 2003. Genetic animal models for absence epilepsy: a review of the WAG/Rij strain of rats. Behav. Genet. 33, 635–655.

Coenen, A.M., Drinkenburg, W.H., Peeters, B.W., Vossen, J.M., Van Luijtelaar, E.L., 1991. Absence epilepsy and the level of vigilance in rats of the WAG/Rij strain. Neurosci. Biobehav. Rev. 15, 259–263.

Danis, O., Demir, S., Günel, A., Aker, R.G., Gülçebi, M., Onat, F., Ogan, A., 2011. Changes in intracellular protein expression in cortex, thalamus and hippocampus in a genetic rat model of absence epilepsy. Brain Res. Bull. 84, 381–388.

De Borman, B., Lakaye, B., Minet, A., Zorzi, W., Vergnes, M., Marescaux, C., Grisar, T., 1999. Expression of mRNA encoding alpha1E and alpha1G subunit in the brain of a rat model of absence epilepsy. Neuroreport 10, 569–574.

Devinsky, O., Vezzani, A., Najjar, S., De Lanerolle, N.C., Rogawski, M.A., 2013. Glia and epilepsy: excitability and inflammation. Trends Neurosci. 36, 174–184.

Di Giovanni, J., Boudkkazi, S., Mochida, S., Bialowas, A., Samari, N., Lévêque, C., Youssouf, F., Brechet, A., Iborra, C., Maulet, Y., Moutot, N., Debanne, D., Seagar, M., El Far, O., 2010. V-ATPase membrane sector associates with synaptobrevin to modulate neurotransmitter release. Neuron 67, 268–279.

Drinkenburg, W.H., Coenen, A.M., Vossen, J.M., Van Luijtelaar, E.L., 1991. Spike-wave discharges and sleep–wake states in rats with absence epilepsy. Epilepsy Res. 9, 218–224.

El Far, O., Seagar, M., 2011. A role for V-ATPase subunits in synaptic vesicle fusion? J. Neurochem. 117, 603–612.

Elenkov, I.J., Wilder, R.L., Chrousos, G.P., Vizi, E.S., 2000. The sympathetic nerve–an integrative interface between two supersystems: the brain and the immune system. Pharmacol. Rev. 52, 595–638.

Fiordelisio, T., Jiménez, N., Baba, S., Shiba, K., Hernández-Cruz, A., 2007. Immunoreactivity to neurofilaments in the rodent anterior pituitary is associated with the expression of alpha 1A protein subunits of voltage-gated Ca2+ channels. J. Neuroendocrinol. 9, 870–881.

Folbergrová, J., Kunz, W.S., 2012. Mitochondrial dysfunction in epilepsy mitochondrion 12, 35–40.

Galic, M.A., Riazi, K., Heida, J.G., Mouihate, A., Fournier, N.M., Spencer, S.J., Kalynchuk, L.E., Teskey, G.C., Pittman, Q.J., 2008. Postnatal inflammation increases seizure susceptibility in adult rats. J. Neurosci. 28, 6904–6913.

Godbout, J.P., Chen, J., Abraham, J., Richwine, A.F., Berg, B.M., Kelley, K.W., Johnson, R.W., 2005. Exaggerated neuroinflammation and sickness behavior in aged mice following activation of the peripheral innate immune system. Faseb J. 19, 1329–1331.

Gottesmann, C., Gandolfo, G., Zernicki, B., 1995. Sleep–waking cycle in chronic rat preparations with brain stem transected at the caudopontine level. Brain Res. Bull. 36, 573–580.

Gygi, S.P., Rochon, Y., Franza, B.R., Aebersold, R., 1999. Correlation between protein and mRNA abundance in yeast. Mol. Cell. Biol. 19, 1720–1730.

Herz, J., Chen, Y., 2006. Reelin, lipoprotein receptors and synaptic plasticity. Nat. Rev. Neurosci. 7, 850–859.

Ikemoto, A., Bole, D.G., Ueda, T., 2003. Glycolysis and glutamate accumulation into synaptic vesicles. Role of glyceraldehyde phosphate dehydrogenase and 3-phosphoglycerate kinase. J. Biol. Chem. 278, 5929–5940.

Kapás, L., Hansen, M.K., Chang, H.Y., Krueger, J.M., 1998. Vagotomy attenuates but does not prevent the somnogenic and febrile effects of lipopolysaccharide in rats. Am. J. Physiol. 274, R406–R411.

Kékesi, K.A., Juhász, G., Simor, A., Gulyássy, P., Szegő, E.M., Hunyadi-Gulyás, E., Darula, Z., Medzihradszky, K.F., Palkovits, M., Penke, B., Czurkó, A., 2012. Altered functional protein networks in the prefrontal cortex and amygdala of victims of suicide. PLoS One 7 (12), e50532.

Klein, J.P., Khera, D.S., Nersesyan, H., Kimchi, E.Y., Waxman, S.G., Blumenfeld, H., 2004. Dysregulation of sodium channel expression in cortical neurons in a rodent model of absence epilepsy. Brain Res. 1000, 102–109.

Kole, M.H., Brauer, A.U., Stuart, G.J., 2007. Inherited cortical HCN1 channel loss amplifies dendritic calcium electrogenesis and burst firing in a rat absence epilepsy model. J. Physiol. 578, 507–525.

Kovács, Z., Kékesi, K.A., Szilágyi, N., Ábrahám, I., Székács, D., Király, N., Papp, E., Császár, I., Szegő, É., Barabás, K., Péterfy, H., Erdei, A., Bártfai, T., Juhász, G., 2006. Facilitation of spike-wave discharge activity by lipopolysaccharides in Wistar Albino Glaxo/Rijswijk rats. Neuroscience 140, 731–742.

Kovács, Z., Czurkó, A., Kékesi, K.A., Juhász, G., 2011. Intracerebroventricularly administered lipopolysaccharide enhances spike-wave discharges in freely moving WAG/Rij rats. Brain Res. Bull. 85, 410–416.
Kovács, Z., Czurkó, A., Kékesi, K.A., Juhász, G., 2012. Neonatal tricyclic antidepressant clomipramine treatment reduces the spike-wave discharge activity of the adult WAG/Rij rat. Brain Res. Bull. 89, 102–107.
Krueger, J.M., 2008. The role of cytokines in sleep regulation. Curr. Pharm. Des. 14, 3408–3416.
Krueger, J.M., Kubillus, S., Shoham, S., Davenne, D., 1986. Enhancement of slow-wave sleep by endotoxin and lipid A. Am. J. Physiol. 251, R591–R597.
Krueger, J.M., Majde, J.A., Rector, D.M., 2011. Cytokines in immune function and sleep regulation. Handb. Clin. Neurol. 98, 229–240.
Kuno, K., Matsushima, K., 1994. The IL-1 receptor signaling pathway. J. Leukoc. Biol. 56, 542–547.
Laflamme, N., Rivest, S., 2001. Toll-like receptor 4: the missing link of the cerebral innate immune response triggered by circulating gram-negative bacterial cell wall components. Faseb J. 15, 155–163.
Lakaye, B., Thomas, E., Minet, A., Grisar, T., 2002. The genetic absence epilepsy rat from Strasbourg (GAERS), a rat model of absence epilepsy: computer modeling and differential gene expression. Epilepsia 43, 123–129.
Lee, J.K., Won, J.-S., Singh, A.K., Singh, I., 2008. Statin inhibits kainic acid-induced seizure and associated inflammation and hippocampal cell death. Neurosci. Lett. 440, 260–264.
Li, Q., Verma, I.M., 2002. NF-kappaB regulation in the immune system. Nat. Rev. Immunol. 2, 725–734.
Lopez, J.L., 2007. Two-dimensional electrophoresis in proteome expression analysis. J. Chromatogr. B Analyt. Technol. Biomed. Life Sci. 849, 190–202.
Lorton, D., Lubahn, C.L., Estus, C., Millar, B.A., Carter, J.L., Wood, C.A., Bellinger, D.L., 2006. Bidirectional communication between the brain and the immune system: implications for physiological sleep and disorders with disrupted sleep. Neuroimmunomodulation 13, 357–374.
Maroso, M., Balosso, S., Ravizza, T., Liu, J., Aronica, E., Iyer, A.M., Rossetti, C., Molteni, M., Casalgrandi, M., Manfredi, A.A., Bianchi, M.E., Vezzani, A., 2010. Toll-like receptor 4 and high-mobility group box-1 are involved in ictogenesis and can be targeted to reduce seizures. Nat. Med. 16 (4), 413–419.
Marouga, R., David, S., Hawkins, E., 2005. The development of the DIGE system: 2D fluorescence difference gel analysis technology. Anal. Bioanal. Chem. 382, 669–678.
Meeren, H.K., Pijn, J.P., Van Luijtelaar, E.L., Coenen, A.M., Lopes da Silva, F.H., 2002. Cortical focus drives widespread corticothalamic networks during spontaneous absence seizures in rats. J. Neurosci. 22, 1480–1495.
Mlodzikowska-Albrecht, J., Steinborn, B., Zarowski, M., 2007. Cytokines, epilepsy and epileptic drugs – is there a mutual influence? Pharmacol. Rep. 59, 129–138.
Murshid, A., Srivastava, A., Kumar, R., Presley, J.F., 2006. Characterization of the localization and function of NECAP 1 in neurons. J. Neurochem. 98, 1746–1762.
Nikitin, A., Egorov, S., Daraselia, N., Mazo, I., 2003. Pathway studio – the analysis and navigation of molecular networks. Bioinformatics 19, 2155–2157.
Novichkova, S., Egorov, S., Daraselia, N., 2003. MedScan, a natural language processing engine for MEDLINE abstracts. Bioinformatics 19, 1699–1706.
Opp, M.R., 2005. Cytokines and sleep. Sleep Med. Rev. 9, 355–364.
Opp, M.R., Born, J., Irwin, M.R., 2007. Sleep and immune system. In: Ader, R. (Ed.), Psychoneuroimmunology. Academic Press, San Diego, pp. 579–618.
Pahl, H.L., 1999. Activators and target genes of Rel/NF-kappaB transcription factors. Oncogene 18, 6853–6866.
Paxinos, G., Watson, C., 1997. The Rat Brain Stereotaxic Coordinates. Academic Press, San Diego.
Polack, P.-O., Guillemain, I., Hu, E., Deransart, C., Depaulis, A., Charpier, S., 2007. Deep layer somatosensory cortical neurons initiate spike-and-wave discharges in a genetic model of absence seizures. J. Neurosci. 27, 6590–6599.
Rapizzi, E., Pinton, P., Szabadkai, G., Wieckowski, M.R., Vandecasteele, G., Baird, G., Tuft, R.A., Fogarty, K.E., Rizzuto, R., 2002. Recombinant expression of the voltage-dependent anion channel enhances the transfer of Ca2+ microdomains to mitochondria. J. Cell Biol. 159, 613–624.
Sarkisova, K., van Luijtelaar, G., 2011. The WAG/Rij strain: a genetic animal model of absence epilepsy with comorbidity of depression. Prog. Neuropsychopharmacol. Biol. Psychiatry 35, 854–876.
Schiffelholz, T., Lancel, M., 2001. Sleep changes induced by lipopolysaccharide in the rat are influenced by age. Am. J. Physiol. Regul. Integr. Comp. Physiol. 280, 398–403.
Schousboe, A., Sickmann, H.M., Bak, L.K., Schousboe, I., Jajo, F.S., Faek, S.A., Waagepetersen, H.S., 2011. Neuron-glia interactions in glutamatergic neurotransmission: roles of oxidative and glycolytic adenosine triphosphate as energy source. J. Neurosci. Res. 89, 1926–1934.
Shandra, A.A., Godlevsky, L.S., Vastyanov, R.S., Oleinik, A.A., Konovalenko, V.L., Rapoport, E.N., Korobka, N.N., 2002. The role of TNF-alpha in amygdala kindled rats. Neurosci. Res. 42, 147–153.
Shevchenko, A., Wilm, M., Vorm, O., Mann, M., 1996. Mass spectrometric sequencing of proteins silver-stained polyacrylamide gels. Anal. Chem. 68, 850–858.
Singh, A.K., Jiang, Y., 2004. How does peripheral lipopolysaccharide induce gene expression in the brain of rats? Toxicology 201, 197–207.
Sinha, S., Patil, S.A., Jayalekshmy, V., Satishchandra, P., 2008. Do cytokines have any role in epilepsy? Epilepsy Res. 82, 171–176.
Suffczynski, P., Kalitzin, S., Lopes Da Silva, F.H., 2004. Dynamics of non-convulsive epileptic phenomena modeled by a bistable neuronal network. Neuroscience 126, 467–484.
Sullivan, J.M., 2011. A surprisingly singular role for endophilin in synaptic vesicle recycling. Neuron 72, 504–505.
Szegő, E.M., Janáky, T., Szabó, Z., Csorba, A., Kompagne, H., Müller, G., Lévay, G., Simor, A., Juhász, G., Kékesi, K.A., 2010. A mouse model of anxiety molecularly characterized by altered protein networks in the brain proteome. Eur. Neuropsychopharmacol. 20, 96–111.
Tobaben, S., Thakur, P., Fernández-Chacón, R., Südhof, T.C., Rettig, J., Stahl, B., 2001. A trimeric protein complex functions as a synaptic chaperone machine. Neuron 31, 987–999.
Tsang, C.W., Estey, M.P., DiCiccio, J.E., Xie, H., Patterson, D., Trimble, W.S., 2011. Characterization of presynaptic septin complexes in mammalian hippocampal neurons. Biol. Chem. 392, 739–749.
Ueta, H., Nagasawa, H., Oyabu-Manabe, Y., Toida, K., Ishimura, K., Hori, H., 2004. Localization of enolase in synaptic plasma membrane as an alphagamma heterodimer in rat brain. Neurosci. Res. 48, 379–386.
Usami, Y., Hatano, T., Imai, S., Kubo, S., Sato, S., Saiki, S., Fujioka, Y., Ohba, Y., Sato, F., Funayama, M., Eguchi, H., Shiba, K., Ariga, H., Shen, J., Hattori, N., 2011. DJ-1 associates with synaptic membranes. Neurobiol. Dis. 43, 651–662.
van de Bovenkamp-Janssen, M.C., Scheenen, W.J., Kuijpers-Kwant, F.J., Kozicz, T., Veening, J.G., van Luijtelaar, E.L., McEnery, M.W., Roubos, E.W., 2004. Differential expression of high voltage-activated Ca2+ channel types in the rostral reticular thalamic nucleus of the absence epileptic WAG/Rij rat. J. Neurobiol. 58, 467–478.
van de Bovenkamp-Janssen, M.C., van der Kloet, J.C., van Luijtelaar, G., Roubos, E.W., 2006. NMDA-NR1 and AMPA-GluR4 receptor subunit immunoreactivities in the absence epileptic WAG/Rij rat. Epilepsy Res. 69, 119–128.
van Luijtelaar, E.L., Coenen, A.M., 1986. Two types of electrocortical paroxysms in an inbred strain of rats. Neurosci. Lett. 70, 393–397.
Vezzani, A., 2005. Inflammation and epilepsy. Epilepsy Curr. 5, 1–6.
Vezzani, A., Moneta, D., Richichi, C., Aliprandi, M., Burrows, S.J., Ravizza, T., Perego, C., De Simoni, M.G., 2002. Functional role of inflammatory cytokines and antiinflammatory molecules in seizures and epileptogenesis. Epilepsia 43, 30–35.
Vezzani, A., Balosso, S., Ravizza, T., 2008a. The role of cytokines in the pathophysiology of epilepsy. Brain Behav. Immun. 22, 797–803.
Vezzani, A., Ravizza, T., Balosso, S., Aronica, E., 2008b. Glia as a source of cytokines: implications for neuronal excitability and survival. Epilepsia 49, 24–32.
Vezzani, A., Aronica, E., Mazarati, A., Pittman, Q.J., 2011a. Epilepsy and brain inflammation. Exp. Neurol., http://dx.doi.org/10.1016/j.expneurol.2011.09.033.
Vezzani, A., Maroso, M., Balosso, S., Sanchez, M.A., Bartfai, T., 2011b. IL-1 receptor/Toll-like receptor signaling in infection, inflammation, stress and neurodegeneration couples hyperexcitability and seizures. Brain Behav. Immun. 25, 1281–1289.
Weiergräber, M., Henry, M., Ho, M.S., Struck, H., Hescheler, J., Schneider, T., 2008. Altered thalamocortical rhythmicity in Ca(v)2.3-deficient mice. Mol. Cell. Neurosci. 39, 605–618.